



Numerical Simulation of Blood Flow in a Stented Aneurysm Using Lattice Boltzmann Method

M. Ahangari, M. Rezazadeh*

Department of Mechanical Engineering, Golpayegan College of Engineering, Isfahan University of Technology, Golpayegan, Iran

ABSTRACT: An aneurysm is a local deformation of a blood vessel caused by high pressure and wall weakness. The rupture of aneurysms leads to a cerebral hemorrhage and severe complications in the patient. Hemorrhagic stroke is one of the common causes of death by cardiovascular diseases and affects 15% of stroke patients worldwide. Recently, stent placement has been considered a promising and minimally invasive technique to prevent the rupture of an aneurysm. Hemodynamic characteristics of the blood flow are affected by the aneurysm geometry and stent properties. In this study, the effect of the stent size and strut shape on the blood flow parameters are investigated numerically. The Lattice Boltzmann Method is used in this simulation since it is convenient for modeling complex fluid flow and transport phenomena based on kinetic theory and statistic physics. The results show that with reduced pore size, speed and momentum in the aneurysm sac decrease, and stent-struts with a rectangular cross-section perform the best. Additionally, the height of the stent is more effective in reducing the blood flow than the width of the stent.

Review History:

Received: May, 15, 2021

Revised: Feb. 22, 2022

Accepted: Mar. 11, 2022

Available Online: Apr. 07, 2022

Keywords:

Aneurysm

Lattice Boltzmann method

Stent

Vorticity

Blood flow

1- Introduction

An aneurysm is the undesirable local deformation of a blood vessel. A swollen aneurysm can put extra pressure on neural tissues and reduce blood flow to the vital regions of the brain. This restricted blood flow can lead to a stroke or tissue damage [1]. The brain hemorrhage due to rupture of the aneurysm can lead to severe complications such as hydrocephalus, rebleeding and cerebral vasospasm with ischemia [2]. Deployment of a flow diverter stent is a perfect treatment to trigger thrombosis inside the aneurysm by changing the local flow characteristics. Hemodynamic parameters, such as pressure distribution, velocity, and shear stresses, play essential roles in the initiation, growth, and rupture of aneurysms.

Due to its limited permeability, the stent modifies the blood flow into the aneurysm [3, 4]. The stent is a flexible cylindrical mesh that fits with the vessel diameter. The treatment success depends on the ability of the stent to maintain the clotting process [5, 6].

Numerical simulations provide a valuable tool to investigate the stented flow parameters to improve the treatment effect resulting from a stent placement. Studies represent that these complex hemodynamic changes occur by placing a stent at the orifice of the aneurysm. The first experimental and clinical studies of this occlusion technique

using stents in carotid aneurysms were done in 1994 [7]. Some experimental and numerical studies have been carried out to clarify the effect of stent placement on the blood flow inside an aneurysm. Various parameters such as porosity and the stent-strut shape affect the pressure and the shear strain rate within an aneurysm. Lieber et al. [8] investigated the effect of the stent size on the hemodynamics of blood flow inside the aneurysm. Their results indicate that stenting significantly reduces intra-aneurysmal vorticity. Also, the mean circulation inside the aneurysm is reduced to less than 3% of its value before stenting. Liou et al. [9] studied the effect of stent shape, helix versus mesh, on hemodynamics parameters inside the aneurysm cavity. The results represented that both stents can induce more favorable changes in the flow inside the aneurysm as well as direction and undulation of wall shear stresses. The helix stent is more favorable than the mesh stent for endovascular treatment.

Computational Fluid Dynamics (CFD) methods can be used to predict the behavior of stents as endovascular treatment of aneurysms. Aenis et al. [10] simulated a 3D model of the stented aneurysm using the finite element method. The results showed that fluid flow inside the aneurysm cavity diminishes considerably in the stented aneurysm. Also, the high-pressure zone at the distal neck and the dome of the aneurysm after stent placement decreases. Hirabayashi et al. [11] investigated the effect of stent structure and position on blood hemodynamics using the lattice Boltzmann method. They also studied the

*Corresponding author's email: M.rezazade@iut.ac.ir



effect of the velocity reduction numerically [12].

Kim et al. [13] used the Lattice Boltzmann method to study the non-Newtonian blood flow inside the aneurysm. They considered the effect of the different stent-strut geometry and different degrees of porosity on the blood flow inside an aneurysm. They represented that by decreasing the stent porosity, the mean vorticity, mean velocity, and shear rate inside the aneurysm cavity are reduced. Dong et al. [14] performed the effect of the blood flow within an aneurysm with various stent-strut shapes. Their results indicated that different parameters such as porosity and stent-strut shape influence the pressure and the shear strain rate inside an aneurysm. They also found out that the circular and elliptical stent-strut shapes minimize the risk of aneurysm rupture. Rectangular and triangular stent-strut shapes prevent the aggregation of platelets.

Phan and Lee [15] studied the effect of strut shape and porosity on the characteristics of non-Newtonian blood flow inside the aneurysm numerically. They reported that stent porosity and stent-strut shape cause the flow reduction into the aneurysm.

In particular, the stent effects on aneurysm circulation depend not only on the stent parameters but also on the aneurysm geometry. Baráth et al. [16] carried out the effect of the stent parameters on the blood flow reduction inside the aneurysm with different neck sizes. They represented that the stent placement is sufficient for the large neck size of the aneurysm. Also, Shishir et al. [17] show that the vortex location and inflow area in the neck is varied significantly with the geometrical parameter of the aneurysm.

Lattice Boltzmann Method (LBM) is suitable for modeling several features that are important to arterial hemodynamics. Zhang et al. [18] used the LBM to model the blood flow inside an aneurysm with different orifice sizes. The results showed that the ratio of the stent pore size to the aneurysm orifice plays an essential role in the blood flow inside an aneurysm. Xu and Lee [19] simulated the blood flow inside an aneurysm using the Lattice Boltzmann method. The findings reported that the stent reduces the size of eddies near the dome of the aneurysm. They observed that the height of the stent could reduce the vortices near the dome more efficiently than its width.

Some studies investigated the effect of the stent on the non-Newtonian blood flow inside the aneurysm. Huang et al. [20] used the LBM to explore the effect of hemodynamic characteristics of the non-Newtonian blood flow inside an aneurysm. They found out that the non-Newtonian model of blood flow is significant for the low porosity of the stent. Lu and Li [21] developed the Lattice Boltzmann method to study the blood flow for several aneurysm sizes. They explored that the maximum wall shear stress value occurred near the reattachment point at the distal end of the aneurysm.

Mokhtar et al. [22] performed four types of stent configuration on real 3D artery bifurcation aneurysm. The results show that the LBM-based simulations are in good agreement with the Particle Image Velocimetry (PIV) experimental findings. Both methods found that the half-

Y(6mm) stent configuration is by far the best configuration for reducing the blood velocity in the vicinity of the aneurysm sac. Also, the half-Y (6mm) stent configuration recorded the highest percentage of velocity reduction and managed to reduce the pressure at the bifurcation region substantially.

Czaja et al. [23] studied the effect of pulsatile flow on the transport of Red Blood Cells (RBCs) and platelets into aneurysm geometries with varying dome-to-neck aspect ratios. They used a two-dimensional LBM for the blood plasma with a Discrete Element Method (DEM) for both RBCs and platelets. They observed that aneurysms are platelet-rich and red blood cell-poor compared to their parental vessel populations. Also, pulsatility does not affect the shear-driven regime aspect ratios.

Afrouzi et al. [24] simulated the blood flow in a created aneurysm in the artery using the Lattice Boltzmann Method. Blood was selected as a non-Newtonian fluid which was simulated with a power-law model. The results showed that the wall shear stress increases with increasing the power-law exponent. In the main artery, the shear stress is lower due to the smaller velocity gradient. Also, it is observed that at a given Reynolds number, the velocity profiles are closer to one another with increasing the Womersley number.

Wang et al. [25] simulated the three-dimensional blood flow in an artery containing an aneurysm by using the immersed boundary-lattice Boltzmann-finite element method. The results represented that Wall Shear Stress (WSS) plays an important role in the formation and development of atherosclerotic plaques in patient coronary arteries.

It is found that CFD simulations will give us insight into the mechanism of blood flow reduction by a stent. The stent is represented by horizontal stent struts across the orifice of the aneurysm. However, it has been reported that the basic vortex pattern is similar in both rigid and distensible saccular Aneurysms [26]. During the diastolic phase, only minor differences could be perceived. Also, cerebral arteries are observed less distensible than large systemic arteries [27, 28]. Therefore, the elasticity of walls causes a small difference in the primary flow pattern with stents. On the other hand, elasticity should be considered when one needs to study the rupture mechanism based on the elasticity or the influence of the pressure on the wall [11]. The vessel walls are assumed to be rigid because some research showed that there is no apparent difference in the vortex pattern between rigid and distensible saccular aneurysms [26].

For simplicity, two-dimensional cerebral aneurysm geometries are considered. The two-dimensional analysis provides the fundamental discussion on the flow pattern in the aneurysm sac. However, a three-dimensional model of asymmetrical aneurysms or branch vessels should be used for clinical simulation. Moreover, pulsation and non-Newtonian flows should be considered in future works to analyze the blood-clotting ability in aneurysms by stent implantation to prevent rupture of aneurysms.

The main goal of this paper is to investigate the effects of stent-strut shape and size on the hemodynamic characteristics in an aneurysm using the Lattice Boltzmann Method.

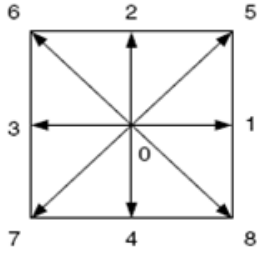


Fig. 1. D2Q9 lattice model

Where $c = \Delta x / \Delta t$, Δx is the lattice spacing, and Δt is the time step. For the case of $\Delta x = \Delta t$, c is taken as 1. The equilibrium distribution f_i^{eq} is expressed as follows [30].

$$f_i^{eq} = w_i \rho \left[1 + \frac{\mathbf{u}_i \cdot \mathbf{e}_i}{c_s^2} + \frac{1}{2} \left(\frac{\mathbf{u}_i \cdot \mathbf{e}_i}{c_s^2} \right)^2 - \frac{1}{2} \frac{\mathbf{u} \cdot \mathbf{u}}{c_s^2} \right] \quad (3)$$

Where $c_s = c / \sqrt{3}$ is the sound speed and w_i is the weighting factor is defined as follows [30].

$$\begin{cases} w_0 = 4/9 \\ w_i = 1/36 & i = 1-4 \\ w_i = 1/9 & i = 5-8 \end{cases} \quad (4)$$

The macroscopic density and momentum are calculated as follows [30]

$$\rho = \sum_{i=1}^8 f_i \quad (5)$$

$$\rho \mathbf{u} = \sum_{i=1}^8 \mathbf{e}_i f_i \quad (6)$$

The kinematic viscosity of the fluid in Navier-Stokes is related to the relaxation time by the following equation [31].

$$\nu = \left(\tau - \frac{1}{2} \right) c_s^2 \Delta t \quad (7)$$

And the pressure p is expressed as:

$$p = c_s^2 \rho \quad (8)$$

The LBM can be split into streaming and collision steps. Thus, Eq. (1) is calculated by the following sequence [31].

The collision step

$$\tilde{f}_i(\mathbf{x}, t) = f_i(\mathbf{x}, t) - \frac{1}{\tau} [f_i(\mathbf{x}, t) - f_i^{eq}(\mathbf{x}, t)] \quad (9a)$$

For simplicity, the blood is considered incompressible, Newtonian, and non-pulsatile. The periodic boundary condition is used at the inlet and outlet, and the bounce-back boundary condition is applied on the wall. The study of fluid mechanical properties in non-stented and stented aneurysmal flow can enable medical experts to evaluate the effectiveness of stent designs and their corresponding porosities in preventing aneurysm dilation leading to rupture.

2- Methods

2- 1- Lattice Boltzmann method

The LBM is a kinetic-based approach for simulating fluid flows. It divides the continuous fluid flow domain into pockets of fluid particles. Fig. 1 shows a 2D model containing nine particles of identical masses, which is known as the D2Q9 model. The D2Q9 is one of the most popular models in two dimensions, in which the discrete lattice Boltzmann equation in classical statistical physics has the following form [30].

$$f_i(\mathbf{x} + \mathbf{e}_i \Delta t, t + \Delta t) - f_i(\mathbf{x}, t) = -\frac{1}{\tau} [f_i(\mathbf{x}, t) - f_i^{eq}(\mathbf{x}, t)] \quad (1)$$

Where $f_i(x, t)$ is the density distribution indicating the particle amount moving in the i th direction with velocity e_i at position x and time t . Δt is the time step, τ is the relaxation time and $f_i^{eq}(x, t)$ is the equilibrium distribution function. The velocity e_i is calculated from the following equation in the two-dimension analysis [30].

$$\mathbf{e}_i = \begin{cases} 0 & i = 0 \\ \left(\cos\left(\frac{\pi(i-1)}{2}\right), \sin\left(\frac{\pi(i-1)}{2}\right) \right) c & i = 1-4 \\ \sqrt{2} \left(\cos\left(\frac{\pi(i-9/2)}{2}\right), \sin\left(\frac{\pi(i-9/2)}{2}\right) \right) c & i = 5-8 \end{cases} \quad (2)$$

Table 1. Simulation parameters[11]

Definition	Symbol	Value
Lattice unit	Δx	5×10^{-5} m
Timestep	Δt	18.5×10^{-6} s
Blood kinematic viscosity	ν_p	3.5×10^{-6} (m ² /s)
Blood density	ρ_p	1060(kg/m ³)
Reynolds number	Re	330
Channel height	D	4×10^{-3} (m)
Channel length	L	4×10^{-2} (m)
Axial pressure gradient	$\partial P / \partial x$	645.7(kg/m ² . s ²)

Table 2. Aneurysm parameters in mm and (lattice unit) [11]

Aneurysm model	Aneurysm parameters		
	Aneurysm diameter, d_a	Aneurysm orifice diameter, d_o	Distance between orifice and center of the aneurysm, h
La	10(200)	10(200)	5.4(108)
Sa	10(200)	5(100)	5.4(108)
Ssa	5(100)	5(100)	2.9(58)

Number in parentheses (lattice unit)

The non-Newtonian behavior of blood affects the viscosity significantly only at low shear rates because the aggregation of the red cells causes the increase of the viscosity at the low shear rates [11]. The influence of shear rates on the viscosity is assumed to be relatively small for vessel diameters more significant than 0.5mm [10, 35]. For tube diameters larger than 0.5 mm, the effect of low shear rates on the behavior of the blood viscosity is considered to be relatively small [35], and inaccuracies resulting from the use of constant viscosity should not be larger than 1 or 2 percent [35]. Additionally, Perktold et al. [27] observed that a comparison between non-Newtonian and Newtonian behavior showed only small differences in the flow phenomena and flow characteristics, which remained virtually constant. In aneurysmal flow, shear rates are generally lower than in the parent vessel; thus, non-Newtonian flow characteristics will differ from the Newtonian flow. However, the focus of this study is on the effects induced by the placement of a stent, and blood viscosity is constant. Also, because the vessel diameter is larger than 1mm (i.e., it falls in the region of high strain rates), the non-Newtonian effect is small, and the flow is assumed to be Newtonian fluid [19]. The body forces such as gravity or boundary forces such as pressure are neglected [5].

The periodic boundary condition combined with velocity and pressure boundaries are used at the inlet and outlet of the channel [36]. Although this will provide simple treatments for inlet and outlet boundaries, realistic flow conditions (e.g., pulsatile flow) are not implemented [19]. The constant pressure gradient rather than a pulsatile flow is used in the present simulation to simplify the study of flow reduction by

stents. In many cases, aneurysmal hemodynamics effects can be investigated from an analysis of steady, non-pulsatile flow, which is simpler and faster to simulate than time-dependent, pulsatile flow [37].

The only difference between the present simulation and that in Ref. [11] is the circular stent-strut shape used by Hirabayashi et al. [11]. In contrast, different stent-strut shapes are used in the current simulation. The vessel diameter is set to 4mm and to ensure that the flow profile is fully developed, the proximal section of the parent artery is set to $10D$, resulting in a length L of 40 mm. The blood flow is assumed as laminar flow.

All the simulation parameters are given in Table 1. The geometric dimensions of the aneurysm and the stent parameters are chosen in the range of experimental data and clinical observations [11]. Two kinds of stent models Ls and Ss are used in the present simulation. The values of the aneurysm and the stent parameters are shown in Fig. 2 are given in Tables 2 and 3, respectively. According to Table 3, two stent models Ls and Ss have different porosity. The porosity of stent model Ls and Ss are 95.51% and 89.53%, respectively. The results of the transient simulation are presented for $t = 0.1$ s.

The main goal of the present research is (i) to study the effects of stent-strut shape; (ii) to study the effects of stent dimension. The current model is utilized to evaluate the effect of stent-strut shape on reducing blood flow inside the aneurysm cavity. The effects of three stent-strut shapes are considered as shown in Fig. 3.

Also, the effect of the dimensions s_f and d_f of a single

Table 3. Stent parameters in mm and (lattice unit) [16]

Stent parameters					
Stent model	Stent diameter, d_s	Filament diameter, d_f	Pore size, s_p	Pore interval, s_f	geometrical porosity, ϵ
Ls	4(80)	0.05(2)	1.75(35)	0.05(2)	95.51
Ss	4(80)	0.05(2)	0.75(15)	0.05(2)	89.53

Number in parentheses (lattice unit)

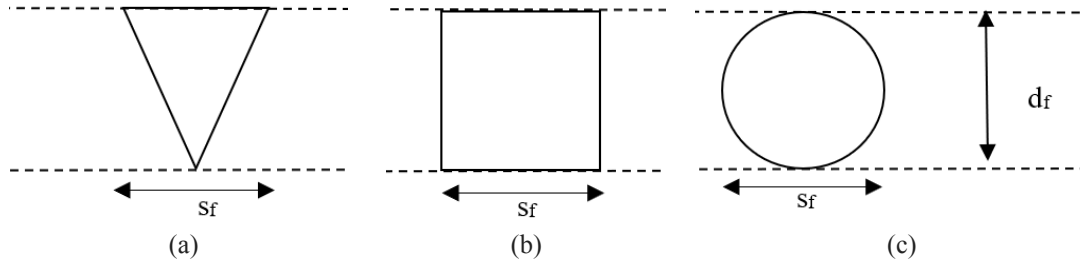


Fig. 3. Stent-strut shape, a) triangular, b) rectangular, c) circular.

Table 4. Single rectangular stent-strut dimensions for different aneurysm model (lattice unit)

Aneurysm model		
Sa	La	Ssa
$d_f = 0.1 \text{ mm}, s_f = 0.1 \text{ mm}$	$d_f = 0.1 \text{ mm}, s_f = 0.1 \text{ mm}$	$d_f = 0.1 \text{ mm}, s_f = 0.1 \text{ mm}$
$d_f = 0.1 \text{ mm}, s_f = 0.3 \text{ mm}$	$d_f = 0.1 \text{ mm}, s_f = 0.3 \text{ mm}$	$d_f = 0.1 \text{ mm}, s_f = 0.3 \text{ mm}$
$d_f = 0.2 \text{ mm}, s_f = 0.1 \text{ mm}$	$d_f = 0.2 \text{ mm}, s_f = 0.1 \text{ mm}$	$d_f = 0.2 \text{ mm}, s_f = 0.1 \text{ mm}$
$d_f = 0.2 \text{ mm}, s_f = 0.3 \text{ mm}$	$d_f = 0.2 \text{ mm}, s_f = 0.3 \text{ mm}$	$d_f = 0.2 \text{ mm}, s_f = 0.3 \text{ mm}$

rectangular stent-strut in Fig. 3 are studied in the three aneurysm models. The dimensions for a single rectangular stent are given in Table 4.

4- Results

4- 1- Verification

A computer program is proposed in FORTRAN to investigate the blood flow inside the aneurysm by the Lattice Boltzmann method. The present simulation used periodic boundary condition at the inlet and outlet, the bounce-back wall boundary condition, viscosity, 0.026, grid resolutions, 800×188 , and the non-dimensional value of pressure gradient, $dp/dx = 4.17 \times 10^{-6}$ to precisely simulate the referred case in [11]. The blood flow velocities at the neck of the aneurysm are compared with Hirabayashi et al. [11] and represented in Fig. 4. The results are in good agreement with the results of Hirabayashi et al. [11].

4- 2- Mesh independency

The mesh-independency is evaluated for a non-stented aneurysm using the model Ssa. The periodic boundary conditions are imposed at the inlet and outlet. The numerical solutions of the fully developed velocity profile are evaluated

at $x=10 \text{ mm}$ and $x=20 \text{ mm}$, as shown in Fig. 5a. The fully developed velocity profiles at the positions mentioned above are represented for three different mesh resolutions in Fig. 5b-c. According to Fig. 5b-c, the mesh 150×640 is sufficient for simulation.

4- 3- Effect of stent shape

Streamlines corresponding to three aneurysm models are shown in Figs. 6 to 8 for non-stented and different stent-strut shapes. Two kinds of stents with different porosities represented in Table 3 are used in the simulation. Stent model Ls with a porosity of 95.51% is used for aneurysm models La and Sa. Also, a stent model of Ss with a porosity of 89.53% is utilized for the aneurysm model Ssa.

According to Figs. 6 to 8, the blood flow into the non-stented aneurysm formed a large vortex near the aneurysm dome. The vortex is significantly reduced as the inserted stent formed a thin boundary layer across the aneurysm neck and reduced the blood flow in the aneurysm sac. Baráth et al. [38] described a significant decrease in the flow velocity after stent implantation. The location of the vortex becomes closer to the center of the aneurysm from the vessel wall, especially for the rectangular stent shape. As shown in Figs. 6 to 8, the

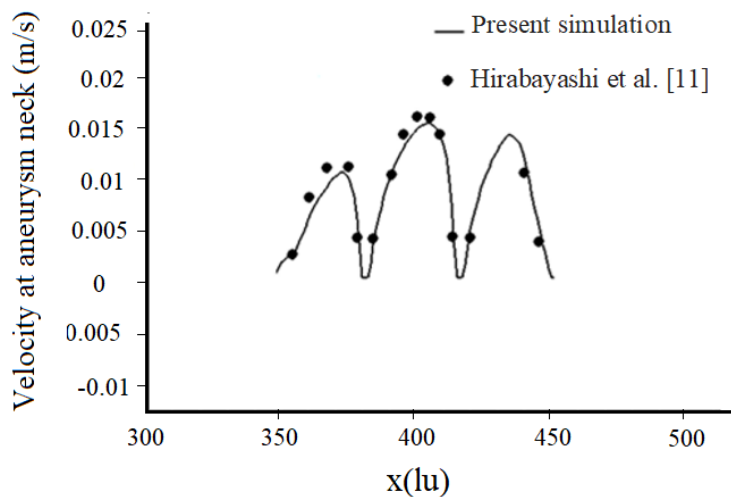


Fig. 4. Velocity magnitude comparison at the neck of the aneurysm

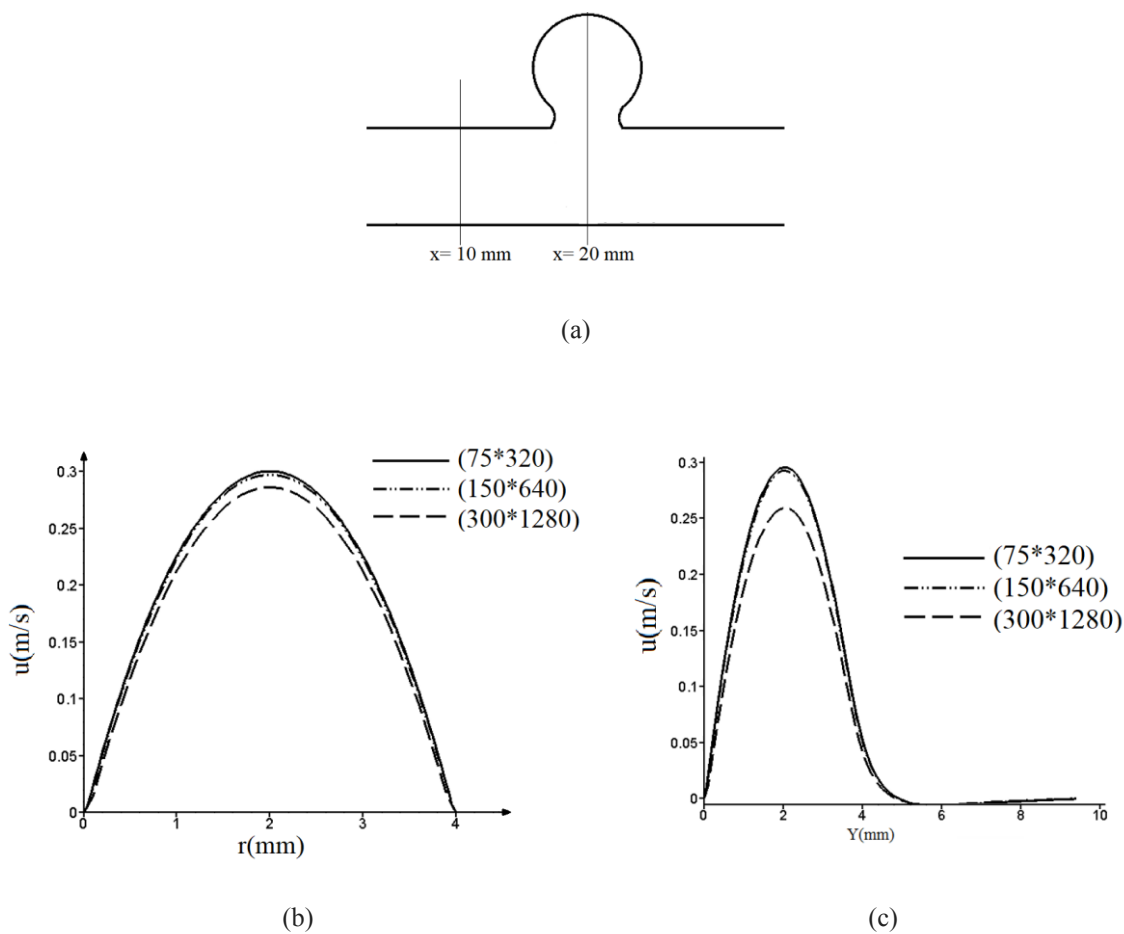


Fig. 5. Fully developed velocity profiles for two cross-sections with a dotted line in (a). The profile in b) $x=10$ mm, c) $x=20$ mm.

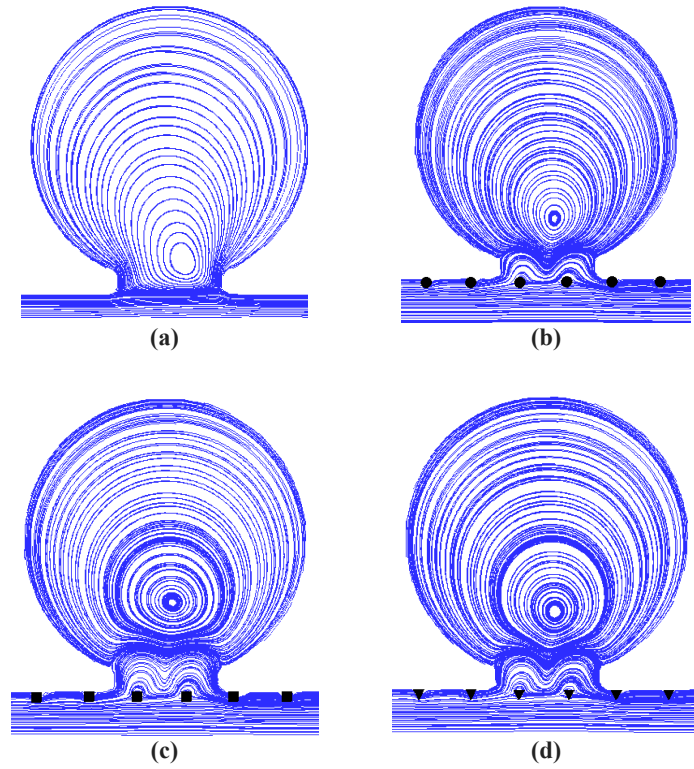


Fig. 6. Streamline inside the aneurysm Sa a) without a stent, with stent model Ls with porosity of 95.51% and different stent-strut shape, b) circular, c) rectangular, d) triangular.

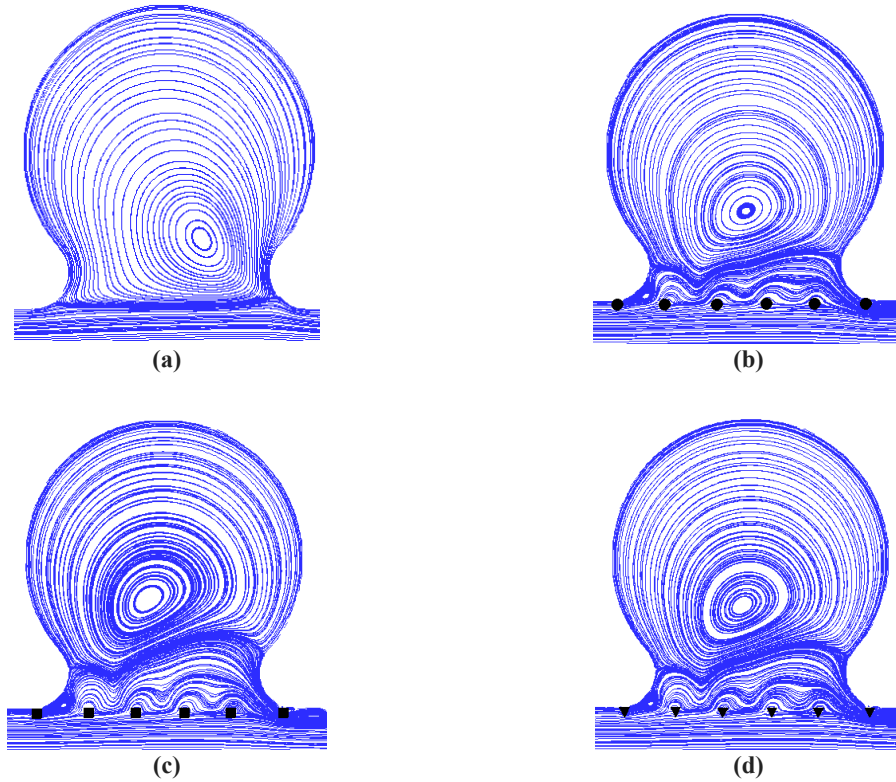


Fig. 7. Streamline inside the aneurysm La a) without a stent, with stent model Ls with porosity of 95.51% and different stent-strut shape, b) circular, c) rectangular, d) triangular.

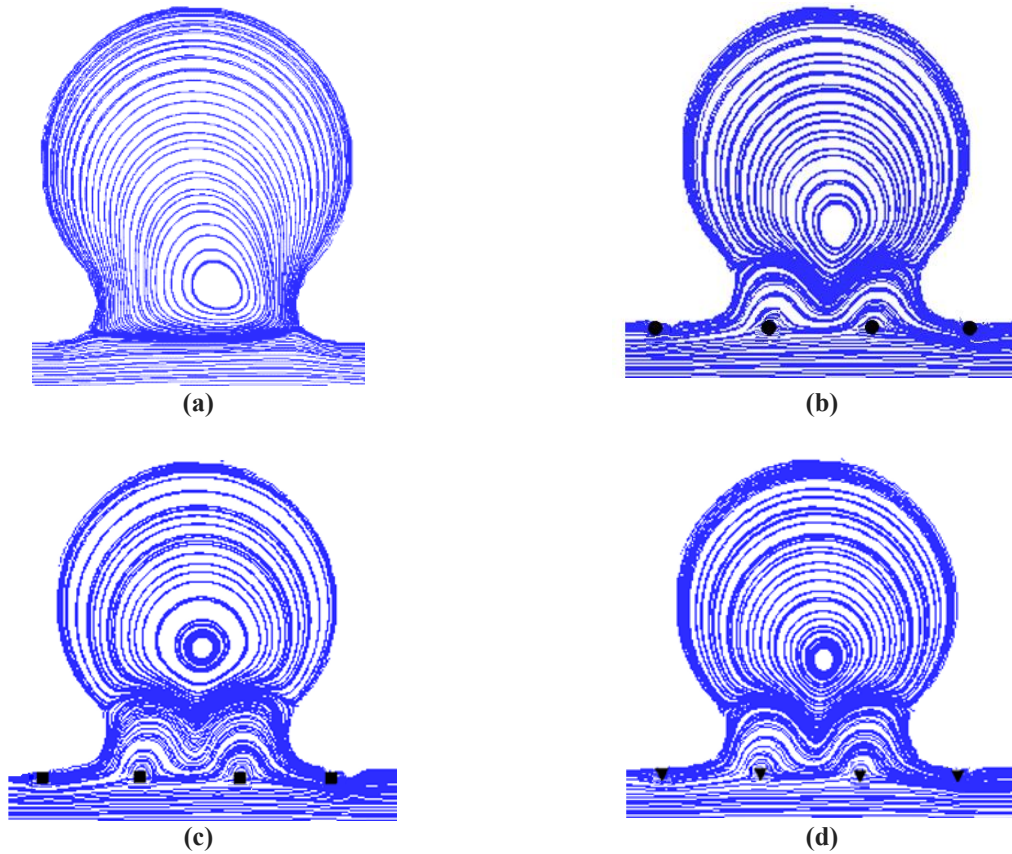


Fig. 8. Streamline inside the aneurysm Ssa a) without a stent, with stent model Ss with porosity of 89.53% and different stent-strut shape, b) circular, c) rectangular, d) triangular.

vortex size in the aneurysm cavity becomes much smaller for all stent-strut shape cases. Also, the smallest size of the vortex corresponds to a rectangular stent-strut shape case. A similar observation was made by Kim et al. [39].

The boundary layer around a rectangular stent is more significant than that formed around triangular and circular stents. Thus, the blood flow into the aneurysm cavity decreases after stent placement. It should be represented that not only the stent-strut shape but also the aneurysm orifice size determines the vortex evolution in the aneurysm. Thus, the flow reduction effect in aneurysms with a small orifice size of model Sa is smaller than that with big orifice size models of La and Ssa.

The maximum non-dimensional flow velocity at the orifice of aneurysm V_o^* is defined as follows.

$$V_o^* = \frac{V_{o \max}}{U} \quad (12)$$

Where $V_{o \max}$ is the maximum velocity at the aneurysm orifice. Moreover, U is the flow velocity at the center of the blood vessel. The mean velocity reduction, V_r , indicates the

effect of the stent on the decrease of total flow velocity and is obtained from Eq. (13).

$$V_r = \frac{V_{ns} - V_{st}}{V_{ns}} \quad (13)$$

Where V_{st} and V_{ns} denote the mean flow velocities in the stented and non-stented aneurysm cavities, respectively. Velocity variation at the orifice of the three mentioned aneurysm models is illustrated in Fig. 9. Maximum non-dimensional flow velocity at the orifice of the aneurysm, average velocity reduction, the vertical component of fluid momentum (ρv), and wall shear stress are given in Table 5.

Fig. 9 and Table 5 demonstrate that the flow velocity at the orifice of an aneurysm diminishes for all stent-strut shapes. Thus, the rectangular stent is more effective than other stent-strut shapes in reducing the blood flow velocity. For the rectangular stent, the Mean velocity reduction for the aneurysm model La is over 77% higher than that of the Sa and Ssa models. Also, the mean velocity reduction of the aneurysm model Ssa is 63% lower than that of the La and Sa models. It is expected that this reduction of mean velocity

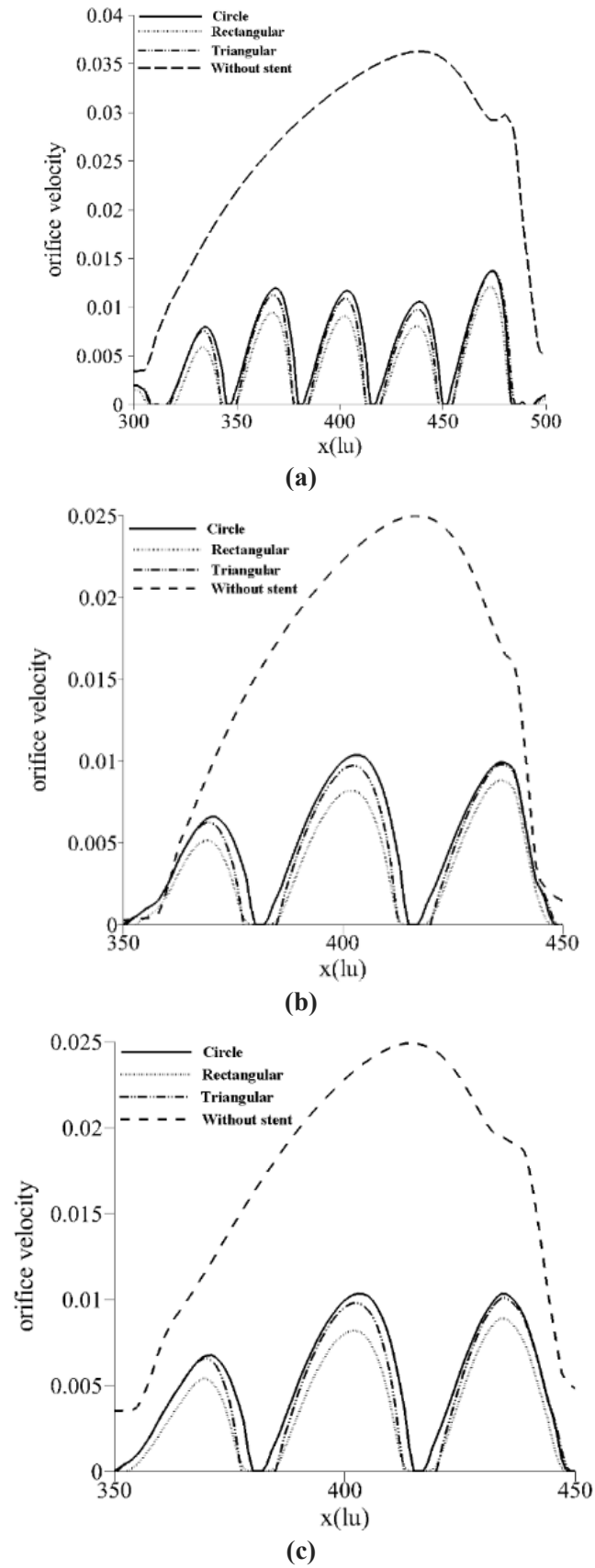


Fig. 9. Velocity variation at the orifice of an aneurysm a) Sa model, b) La model, c) Ssa model.

Table 5. Measured parameters in the simulation for different stent shape

Model	Stent shape	V_0^*max	Momentum, ρv (kg/m ² s)	mean velocity, reduction, $V_r(\%)$	Vorticity, w (1/s)	Wall shear stress (Pa)
Sa	Circular	0.077	0.548	67	0.337	0.001250270
	Rectangular	0.062	0.343	74	0.272	0.001009120
	Triangular	0.07	0.426	71	0.338	0.001253980
La	Circular	0.111	1.561	70	0.189	0.000701190
	Rectangular	0.0983	0.826	77	0.172	0.000638120
	Triangular	0.111	1.142	73	0.196	0.000727160
Ssa	Circular	0.076	1.085	57	0.302	0.001120420
	Rectangular	0.0634	0.857	63	0.248	0.000920080
	Triangular	0.071	0.679	60	0.294	0.001090740

promotes the occurrence of hemostasis inside the aneurysm. Thus, the risk of the growth or possible rupture of the vessel will be decreased.

According to Table 5, the momentum transfer into the aneurysm dome diminishes considerably for all cases after stent placement. Moreover, the most significant reduction of momentum at the center of the aneurysm corresponds to the rectangular stent. For the rectangular stent, the maximum value of momentum reduction is 92% in the La model. This is in good agreement with the results of Kim et al. [39]. Also, the smallest value of momentum reduction is 69% in the Ssa model for the circular stent.

As given in Table 5, the rectangular stent reduced the momentum moving into the aneurysm considerably. Moreover, the circular stent is ineffective, and the triangular stent created a moderate change. Therefore, the value of the force exerted on the aneurysm dome is minimized for the rectangular stent-strut shape. The vorticity is defined as follows.

$$w = \frac{\partial v}{\partial x} - \frac{\partial u}{\partial y} \quad (14)$$

In which u and v are velocity components in the x and y -direction, respectively. Maximum amounts of vorticity inside an aneurysm cavity are given in Table 5. As given in Table 4, the strength of vortices in all three aneurysm models diminishes for all stent-strut shapes.

The vorticity in the aneurysm cavity is reduced due to a decrease in the shear stress, and flow stagnancy, and the induction of thrombosis increases. These undesirable conditions will aggravate aneurysm rupture [39]. Therefore, the type of stents employed must have sufficient porosity to minimize aneurysmal rupture [40].

According to Table 5, WSS values at the aneurysm dome are small in all stented aneurysm models due to the small

velocity values. The small WSS values at the aneurysm dome are represented by Ohta et al. [41]. The magnitude of wall shear stress of the stented aneurysm is reduced, particularly in the zone close to the distal neck [42]. Experimental and numerical studies confirm that a high wall shear stress (> 40.0 Pa) is regarded as a significant factor in the initiation of a cerebral aneurysm [43, 44]. In comparison, a low WSS (< 2.0 Pa) might be a significant factor in its growth and rupture [45]. Measurements of quantities of interest, such as shear stress, are challenging to make in vivo [19]. Thus, numerical simulation becomes a suitable tool for studying the effect of WSS.

According to Fig. 9 and Table 5, a rectangular stent causes a significant reduction of the velocity gradient due to a thicker boundary layer at the orifice of the aneurysm. Moreover, the circular and triangular stents reduced the vorticity moderately. High shear stress is required to prevent blood clotting. Thus, using the rectangular stent will minimize the risk of aneurysm rupture. Triangular, and circular stents are more suitable for preventing the accumulation of blood platelets.

Figs. 10 to 12 represent the blood pressure, and velocity field corresponding to three aneurysm models. According to Figs. 10 to 12, a high-pressure zone at the distal neck and the dome of the aneurysm before tenting decreases after stent placement for all stent-strut shapes [10]. The stent modifies the blood pressure and velocity profiles on both the vessels and the aneurysm.

In particular, the pressure decreases at the downstream areas of the aneurysm after stent placement which is in good agreement with previous numerical results of Ouared and Chopard [46].

Also, the velocity is significantly affected by strut shapes. The reduction in velocity demonstrated less flow near the aneurysm dome, which indicated that inserted stents created less pressure near the aneurysm dome. However, the vortex in the stented aneurysm is not caused by the pressure difference in the aneurysm because the velocity magnitude at the orifice is not enough to drive the flow.

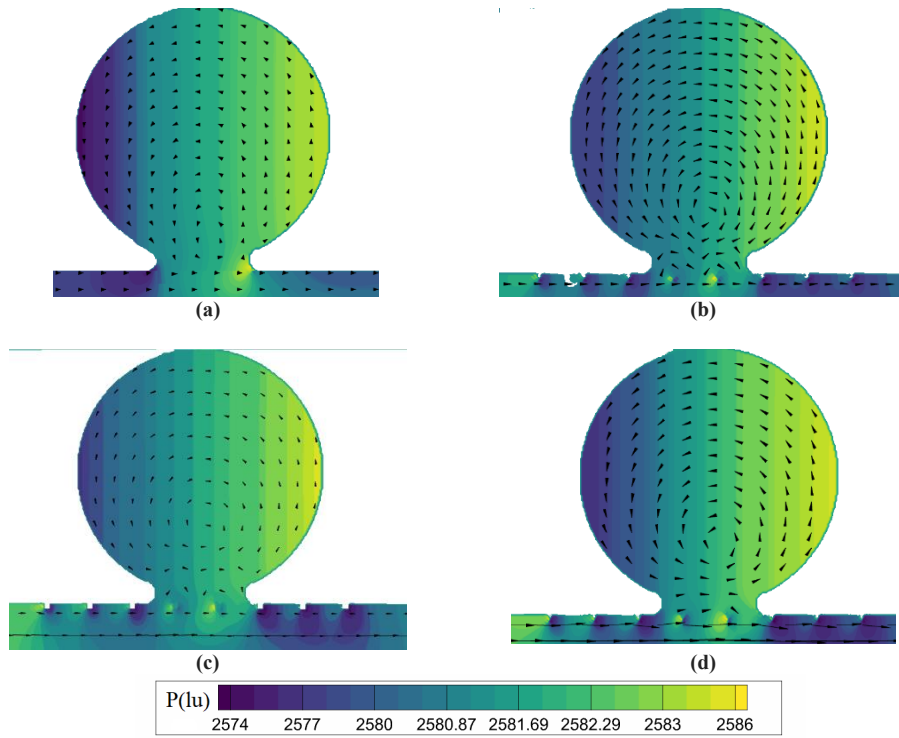


Fig. 10. Blood pressure and velocity field inside the aneurysm Sa a) without stent, with stent model Ls with porosity of 95.51% and different stent-strut shape, b) circular, c) rectangular, d) triangular.

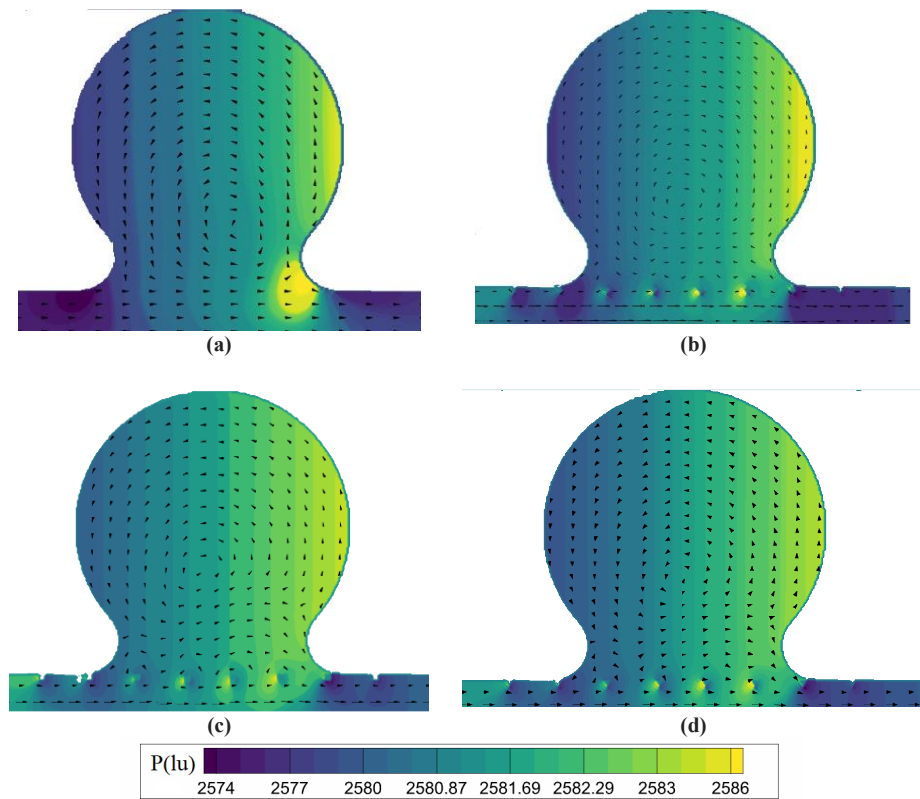


Fig. 11. Blood pressure and velocity field inside the aneurysm La a) without stent, with stent model Ls with porosity of 95.51% and different stent-strut shape, b) circular, c) rectangular, d) triangular.

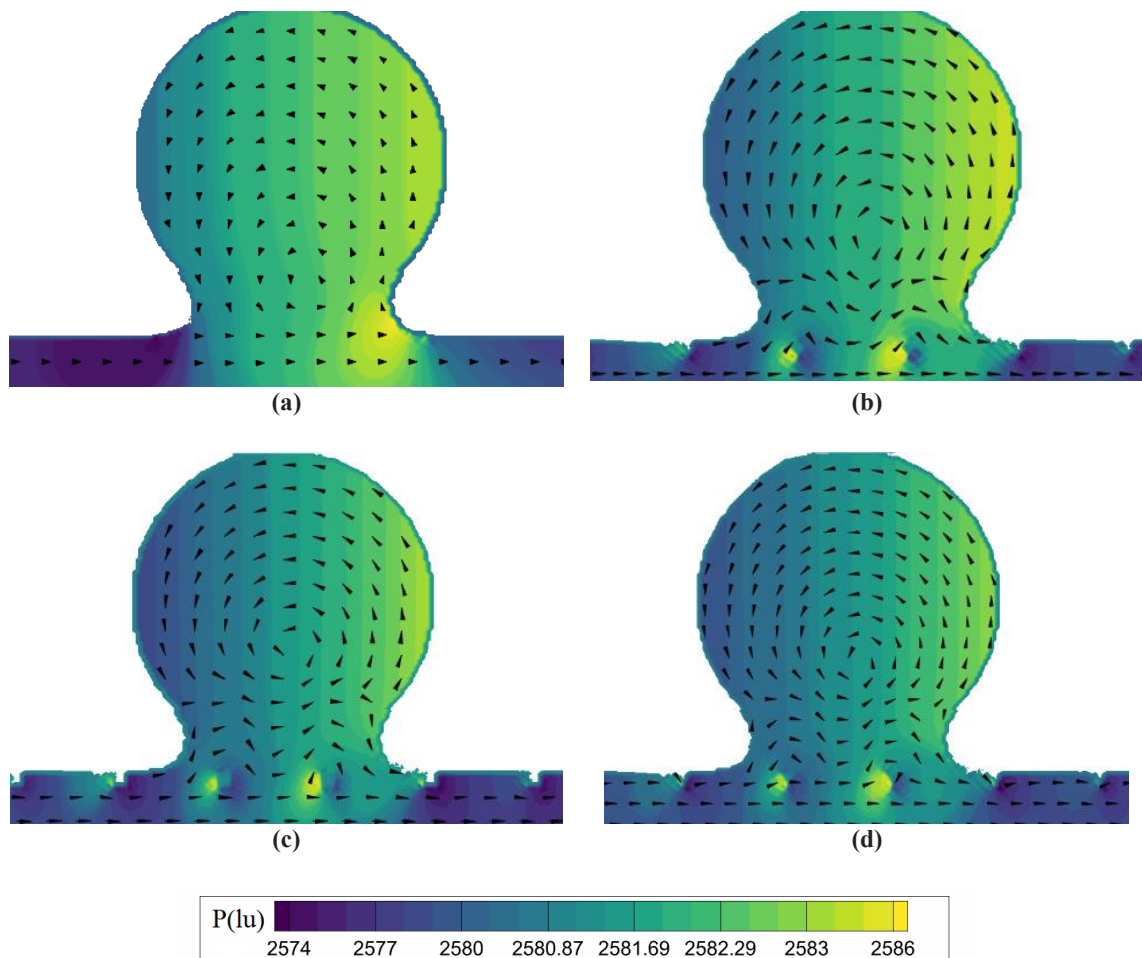


Fig. 12. Blood pressure and velocity field inside the aneurysm Ssa a) without stent, with stent model Ss with porosity of 89.53% and different stent-strut shape, b) circular, c) rectangular, d) triangular.

4- 4- Effect of stent dimensions

As mentioned before, rectangular stents cause a significant reduction in the flow into the aneurysm. Thus, the flow in aneurysms with a simple ring-shaped stent obstacle is simulated to study the flow inside the aneurysm. The ring-shaped stent obstacle is placed normal to the main flow direction. Thus, the effect of the dimensions of a rectangular stent obstacle is investigated in the three aneurysm models. Since aneurysm rupture usually occurs at the apex of the dome [19, 47], the effect of the stent location near the aneurysm dome is studied. The dimensions used for a rectangular stent obstacle are given in Table 6. The streamlines in the three aneurysm models for a rectangular stent obstacle with

different dimensions are shown in Figs. 13 to 15.

According to Table 6, the size of the vortices diminishes considerably for stented Ssa aneurysm. The blood flow moved into the non-stented aneurysm sac without any blocking, thus a large vortex size is created in the aneurysm sac. However, the vortex size was decreased by the stent implementation inside the aneurysm.

According to Figs. 13 to 15 and Table 6, the stent height is more efficient in the flow pattern, and the vortices move from the cavity to the orifice of the aneurysm, which is in good agreement with that obtained by Xu and Lee [19]. On the other hand, the increase of stent width has less effect on the flow pattern for all models of aneurysms. According to Table 6,

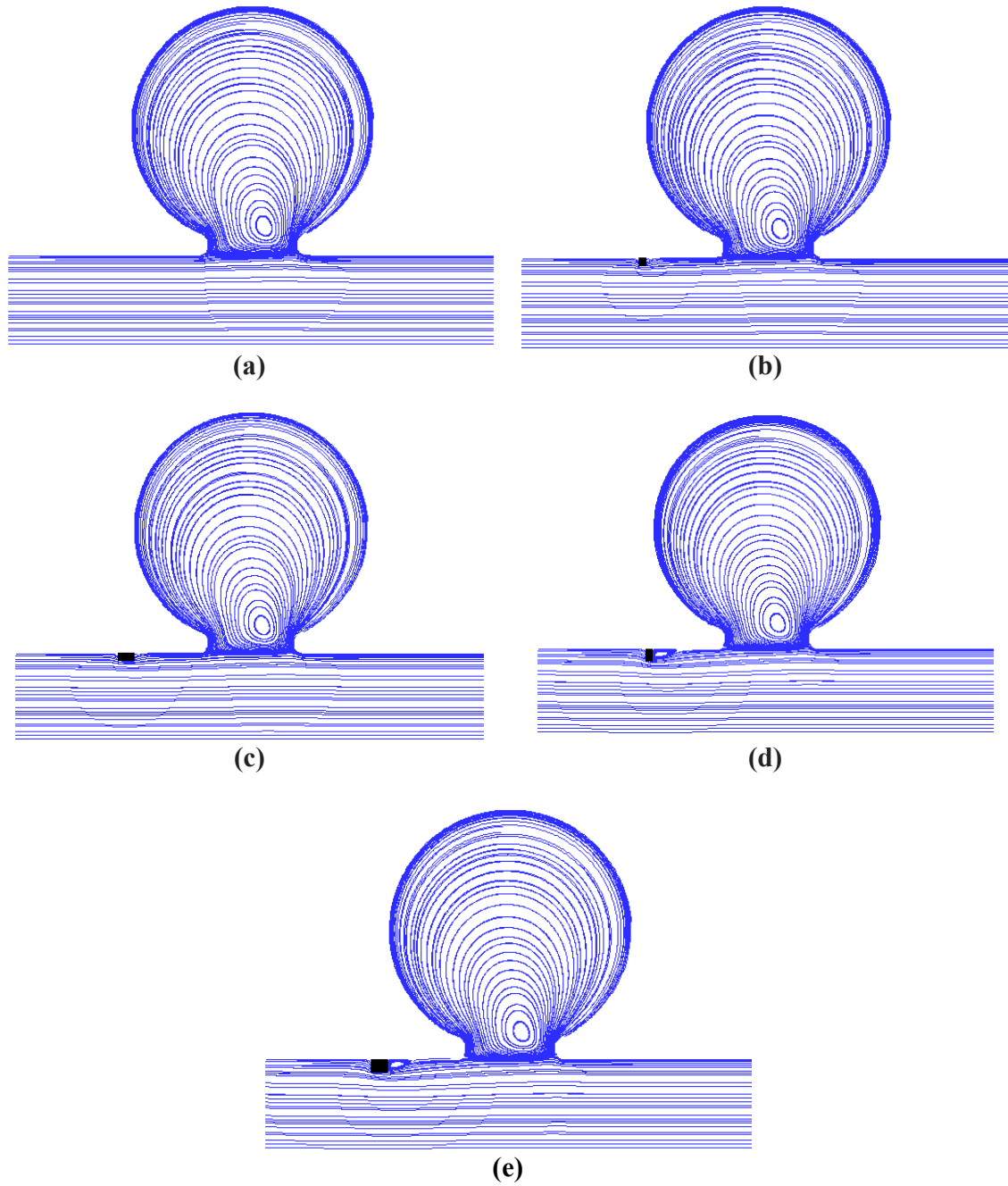


Fig. 13. streamline inside the aneurysm model of Sa , a) without stent, b) $df = 0.1, sf = 0.1$, c) $df = 0.1, sf = 0.2$, d) $df = 0.2, sf = 0.1$, e) $df = 0.2, sf = 0.3$.

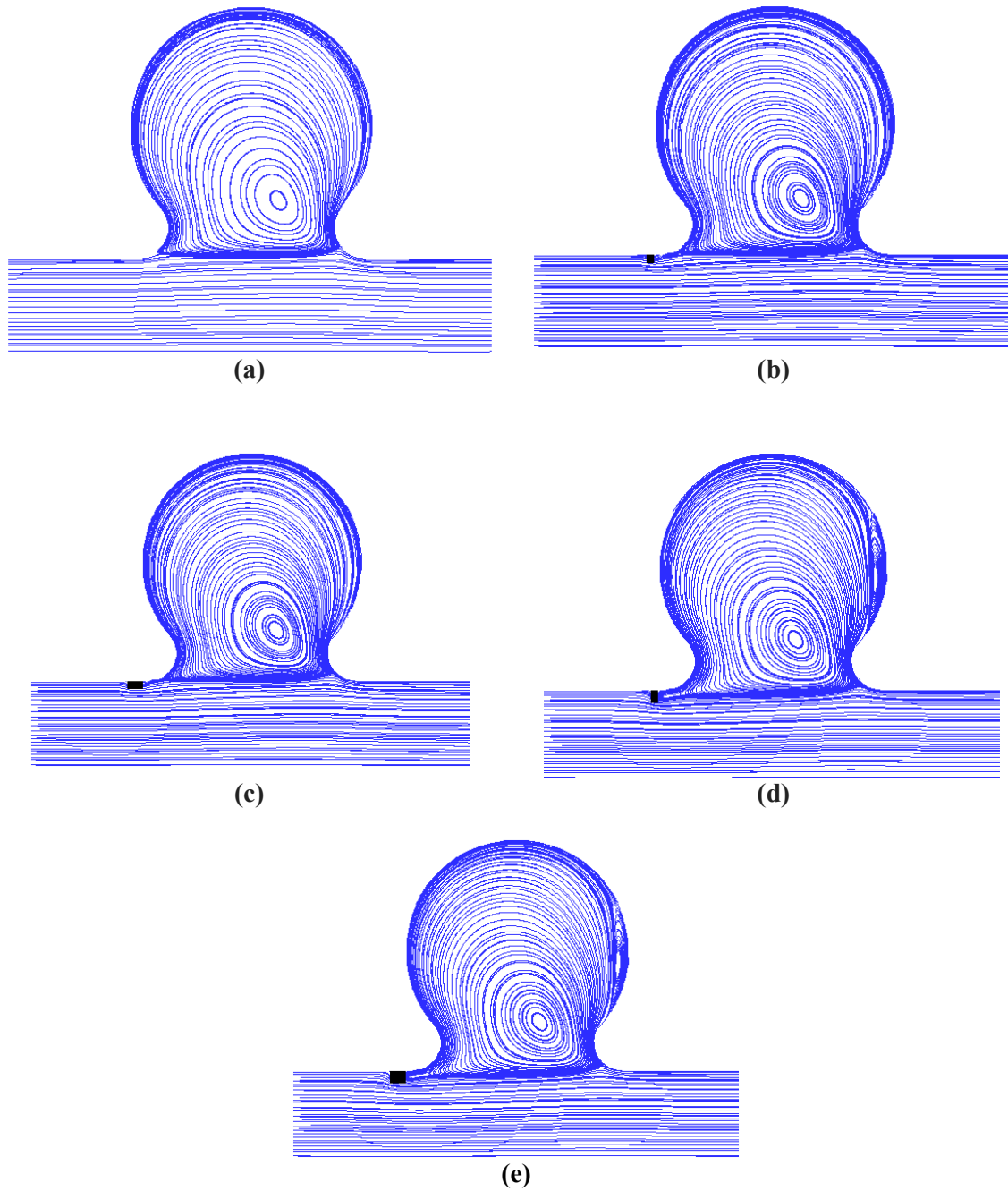


Fig. 14. streamline inside the aneurysm model of La, a) without stent, b) $df=0.1, sf=0.1$, c) $df=0.1, sf=0.2$, d) $df=0.2, sf=0.1$, e) $df=0.2, sf=0.3$.

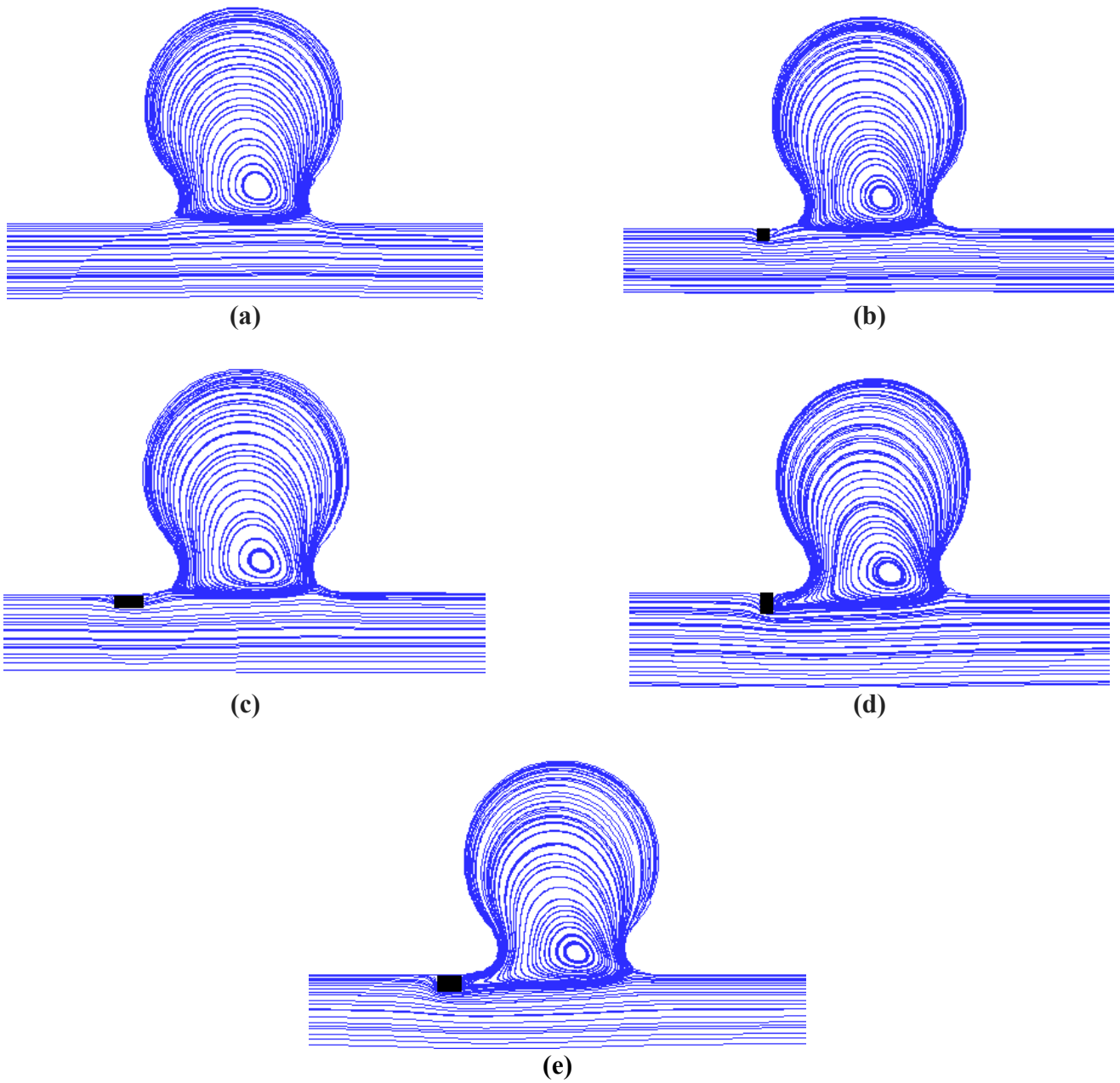


Fig. 15. streamline inside the aneurysm model of Ssa, a) without stent, b) $df=0.1$, $sf=0.1$, c) $df=0.1$, $sf=0.2$, d) $df=0.2$, $sf=0.1$, e) $df=0.2$, $sf=0.3$.

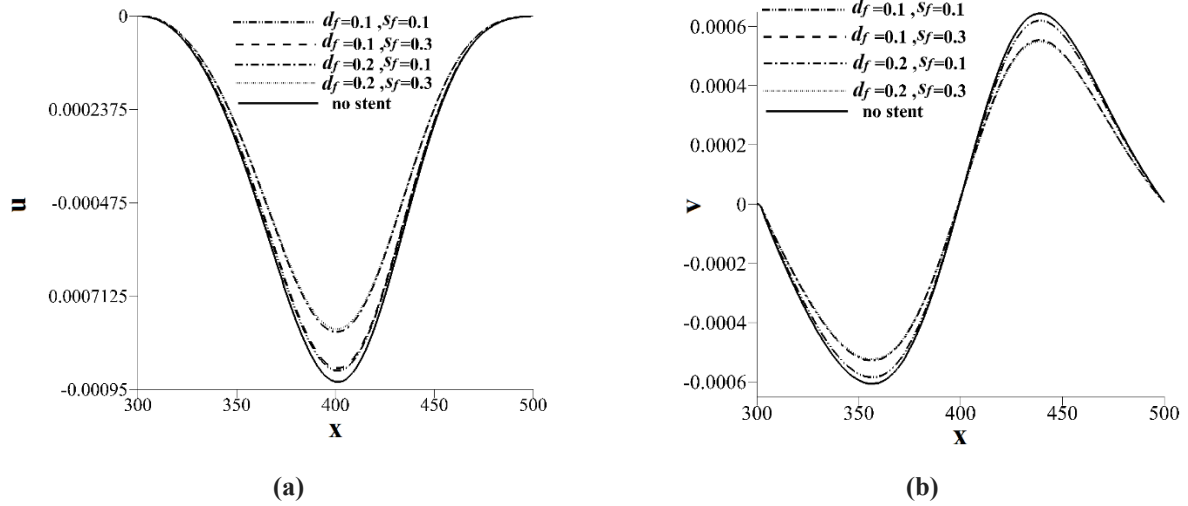


Fig. 16. Velocity in the center of aneurysm model of Sa, a) x component, b) y component.

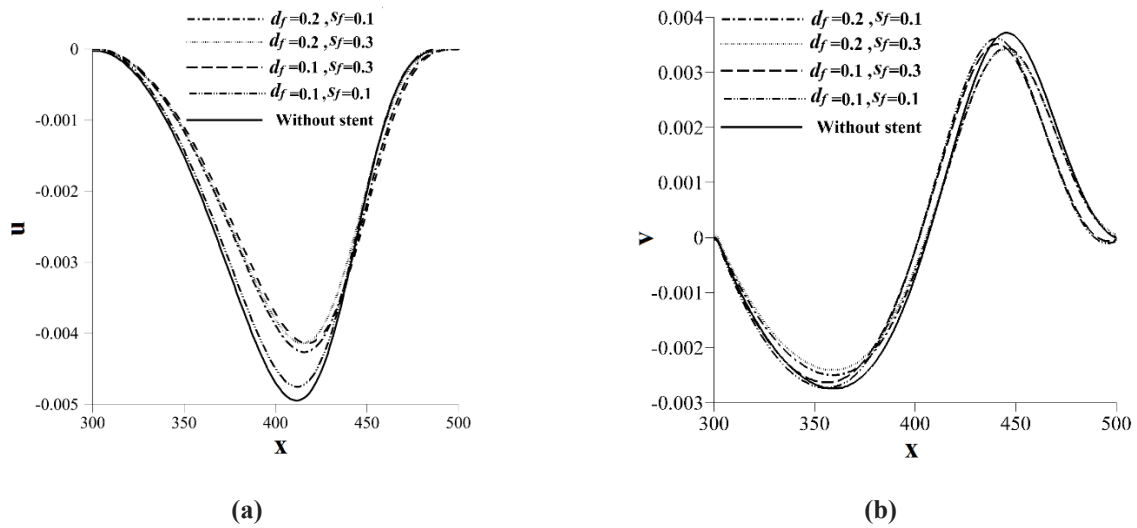


Fig. 17. Velocity in the center of aneurysm model of La, a) x component, b) y component.

the average velocity reductions in the cavity of Sa, La, and Ssa aneurysm models for $d_f = 0.2$ and $s_f = 0.3$ are 13.89%, 11.74%, and 12.82%, respectively. The most reduction for all aneurysm models corresponds to $d_f = 0.2$ and $s_f = 0.3$. The most reduction of vorticity corresponds to the Ssa model for $d_f = 0.2$ and $s_f = 0.3$. Consequently, the increase of stent width, compared to its height, exerts very little influence on the velocity fluctuations at the cavity and orifice of the aneurysm.

Figs. 16 to 18 illustrate the velocity variation at the center of the aneurysm for rectangular stents with various dimensions. The velocity components at the center of the aneurysm diminish by placing a rectangular stent, which indicates the flow reduction in the aneurysm dome. Maximum velocity reduction corresponds to the rectangular stent with $d_f = 0.2$ and $s_f = 0.3$. The stent height is a more effective parameter

than stent width in reducing the blood flow velocity at the dome of the aneurysm. Thus, the effect of stent width can be disregarded. The velocity reduction in the y -direction indicated less flow near the aneurysm dome, which predicted less pressure near the stented aneurysm dome.

According to Table 5, the most momentum reduction occurs in the rectangular stent with dimensions $d_f = 0.2$ and $s_f = 0.3$. The rectangular stent reduced the momentum moving into the Sa aneurysm model significantly. The increase of stent width has no significant effect on the momentum at the aneurysm center. On the other hand, the momentum at the aneurysm center diminishes considerably as the stent height increase and, the risk of the rupture of the aneurysm is reduced.

The value of vorticity is higher at the orifice of the

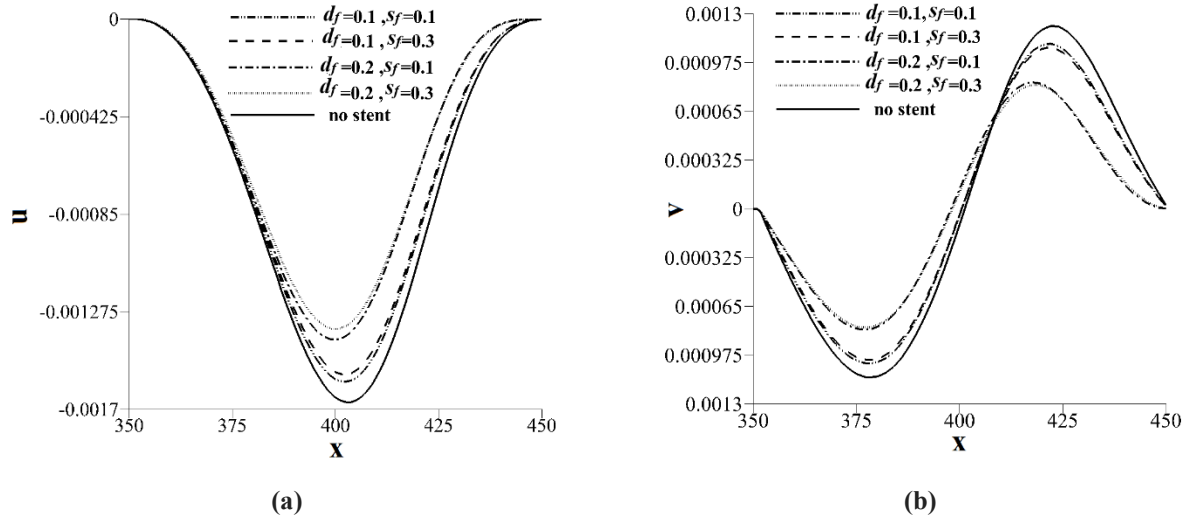


Fig. 18. Velocity in the center of aneurysm model of Ssa, a) x component, b) y component.

Table 6. Measured parameters in the simulation for different stent dimension

Model	V_0^*	Mean velocity reduction, V_r	Momentum, ρv (kg/m ² s)	Vorticity (1/s)	ω_w	Wall shear stress (Pa)
Without stent	0.19	0	1.786	0.695		0.00250796
Sa	$d_f=0.1$ mm, $s_f=0.1$ mm	0.188	2.82	1.772	0.676	0.00249312
	$d_f=0.1$ mm, $s_f=0.3$ mm	0.168	3.52	1.585	0.672	0.00216664
	$d_f=0.2$ mm, $s_f=0.1$ mm	0.166	12.44	1.572	0.584	0.00217777
	$d_f=0.2$ mm, $s_f=0.3$ mm	0.195	13.189	1.834	0.587	0.00257845
Without stent	0.284	0	9.424	0.838		0.00291235
La	$d_f=0.1$ mm, $s_f=0.1$ mm	0.282	1.711	9.341	0.785	0.00288267
	$d_f=0.1$ mm, $s_f=0.3$ mm	0.235	2.46	8.842	0.777	0.002338042
	$d_f=0.2$ mm, $s_f=0.1$ mm	0.234	10.63	8.733	0.6302	0.00234101
	$d_f=0.2$ mm, $s_f=0.3$ mm	0.305	11.74	9.828	0.631	0.00310898
Without stent	0.16	0	3.145	0.618		0.00190323
Ssa	$d_f=0.1$ mm, $s_f=0.1$ mm	0.156	7.02	3.072	0.513	0.001855
	$d_f=0.1$ mm, $s_f=0.3$ mm	0.102	8.76	2.413	0.5	0.00099428
	$d_f=0.2$ mm, $s_f=0.1$ mm	0.101	9.11	2.359	0.268	0.00100541
	$d_f=0.2$ mm, $s_f=0.3$ mm	0.187	12.82	3.486	0.271	0.00229278

aneurysm. The vorticity amount diminishes by approaching the aneurysm center, because the velocity gradient decreased. In contrast, the larger velocity gradient occurs near aneurysm walls causing a significant increase in the shear stresses and vorticity. The most vorticity reductions, relative to the non-stented case, occurred for a rectangular stent with dimensions $d_f=0.1$ and $s_f=0.1$ in all aneurysm models. The magnitude of vorticity reduction is 15.91%, 24.86%, and 56.5% for Sa; La; and Ssa aneurysm models, respectively. The increase in stent height has a significant effect on vorticity. Thus, the amount of vorticity diminishes by increasing the stent height.

5- Conclusion

In this paper, a two-dimensional numerical analysis of the flow pattern in the stented aneurysm is presented using the Lattice Boltzmann method. The effect of the size and shape of the stent on the hydrodynamic parameters of blood flow are studied. The stent is assumed to be a solid obstacle along with the aneurysm orifice, and blood is considered a Newtonian incompressible fluid. Three shapes of stent rectangle, circle, and triangle with the same d_f and s_f are considered.

The results represent that vorticity, shear stress, maximum velocity, and momentum are decreased in the stented

aneurysms. Also, the height of the stent is more efficient than its width in reducing the blood flow. The most reduction corresponds to a rectangular stent with $d_f=0.2$ mm, $s_f=0.3$ mm. In this case, the average velocity reduction for Ssa, Sa, and La are 12%, 13%, and 11%, respectively. Also, the most vorticity reduction in all aneurysm models is observed for a rectangular stent with dimensions $d_f = 0.2$ mm and $s_f = 0.1$ mm. In this case, the vorticity reduction is 15.91%, 24.86%, and 56.5% for Sa; La, and Ssa aneurysm models, respectively.

The study of fluid mechanical properties in stented aneurysmal flow can enable medical experts to evaluate the effectiveness of stent designs in preventing aneurysm dilation leading to rupture.

6- Limitations

Based on the limitations of the present study, a more simplified model based on the LBM approach is used to simulate the blood flow inside the stented aneurysm. The first limitation is that more accurate hemodynamic results can be gained by using an elastic model than a rigid one. The second limitation is that the present study used a Newtonian working fluid. Also, blood is a non-Newtonian fluid, in vessels larger than 0.5 mm in diameter, it is considered to behave as a Newtonian fluid [29]. The last limitation of the present study is that the analysis is performed only in the symmetrical plane of the sac, which is insufficient to reproduce a real-life 3D configuration of the flow. However, the 2D approach is appropriate for comparing the stented and non-stented situations in different models of the aneurysm.

References

- [1] D. Scheinert, M. Schroder, H. Steinkamp, J. Ludwig, G. Biamino, Treatment of iliac artery aneurysms by percutaneous implantation of stent grafts, *Circulation*, 102(suppl_3) (2000) Iii-253-Iii-258.
- [2] I. Wanke, A. Dörfler, M. Forsting, Intracranial aneurysms, in: *Intracranial vascular malformations and aneurysms*, Springer, 2008, pp. 167-283.
- [3] G. Geremia, M. Haklin, L. Brennecke, Embolization of experimentally created aneurysms with intravascular stent devices, *American Journal of Neuroradiology*, 15(7) (1994) 1223-1231.
- [4] M. Hirabayashi, M. Ohta, D.A. Rüfenacht, B. Chopard, Characterization of flow reduction properties in an aneurysm due to a stent, *Physical Review E*, 68(2) (2003) 021918.
- [5] F. Turjman, T.F. Massoud, C. Ji, G. Guglielmi, F. Vi, J. Robert, Combined stent implantation and endosaccular coil placement for treatment of experimental wide-necked aneurysms: a feasibility study in swine, *American Journal of Neuroradiology*, 15(6) (1994) 1087-1090.
- [6] A.K. Wakhloo, F. Schellhammer, J. de Vries, J. Haberstroh, M. Schumacher, Self-expanding and balloon-expandable stents in the treatment of carotid aneurysms: an experimental study in a canine model, *American Journal of Neuroradiology*, 15(3) (1994) 493-502.
- [7] M.P. Marks, M.D. Dake, G.K. Steinberg, A.M. Norbash, B. Lane, Stent placement for arterial and venous cerebrovascular disease: preliminary experience, *Radiology*, 191(2) (1994) 441-446.
- [8] B.B. Lieber, V. Livescu, L. Hopkins, A.K. Wakhloo, Particle image velocimetry assessment of stent design influence on intra-aneurysmal flow, *Annals of biomedical engineering*, 30(6) (2002) 768-777.
- [9] T.-M. Liou, S.-N. Liou, K.-L. Chu, Intra-aneurysmal flow with helix and mesh stent placement across side-wall aneurysm pore of a straight parent vessel, *J. Biomech. Eng.*, 126(1) (2004) 36-43.
- [10] M. Aenis, A. Stancampiano, A. Wakhloo, B. Lieber, Modeling of flow in a straight stented and nonstented side wall aneurysm model, (1997).
- [11] M. Hirabayashi, M. Ohta, D.A. Rüfenacht, B. Chopard, A lattice Boltzmann study of blood flow in stented aneurysm, *Future Generation Computer Systems*, 20(6) (2004) 925-934.
- [12] M. Hirabayashi, M. Ohta, D.A. Rüfenacht, B. Chopard, Lattice Boltzmann analysis of the flow reduction mechanism in stented cerebral aneurysms for the endovascular treatment, in: *International Conference on Computational Science*, Springer, 2003, pp. 1044-1053.
- [13] Y.H. Kim, S. Farhat, X. Xu, J.S. Lee, A lattice Boltzmann study of the non-Newtonian blood flow in stented aneurysm, in: *2008 NSTI Nanotechnology Conference and Trade Show, NSTI Nanotech 2008 Joint Meeting, Nanotechnology 2008*, 2008, pp. 417-420.
- [14] J. Dong, K.K. Wong, Z. Sun, J. Tu, Numerical analysis of stent porosity and strut geometry for intra-saccular aneurysmal flow, in: *2011 Computing in Cardiology*, IEEE, 2011, pp. 477-480.
- [15] D.T. Phan, S.-W. Lee, Effect of Stent Design Porosity on Hemodynamics Within Cerebral Aneurysm Model: Numerical Analysis, *Transactions of the Korean Society of Mechanical Engineers B*, 38(1) (2014) 63-70.
- [16] K. Baráth, F. Cassot, J.H. Fasel, M. Ohta, D.A. Rüfenacht, Influence of stent properties on the alteration of cerebral intra-aneurysmal haemodynamics: flow quantification in elastic sidewall aneurysm models, *Neurological Research*, 27(sup1) (2005) 120-128.
- [17] S.S. Shishir, M.A.K. Miah, A.S. Islam, A.T. Hasan, Blood Flow Dynamics in Cerebral Aneurysm-A CFD Simulation, *Procedia Engineering*, 105 (2015) 919-927.
- [18] X.-j. Zhang, X. Li, F. He, Numerical simulation of blood flow in stented aneurysm using lattice Boltzmann method, in: *7th Asian-Pacific Conference on Medical and Biological Engineering*, Springer, 2008, pp. 113-116.
- [19] X. Xu, J.S. Lee, Application of the lattice Boltzmann method to flow in aneurysm with ring-shaped stent obstacles, *International journal for numerical methods in fluids*, 59(6) (2009) 691-710.
- [20] C. Huang, Z. Chai, B. Shi, Non-newtonian effect on hemodynamic characteristics of blood flow in stented cerebral aneurysm, *Communications in Computational Physics*, 13(3) (2013) 916-928.
- [21] L. Xiao-Yang, Y. Hou-Hui, C. Ji-Yao, F. Hai-Ping, Lattice BGK simulations of the blood flow in elastic vessels, *Chinese Physics Letters*, 23(3) (2006) 738.
- [22] N.H. Mokhtar, A. Abas, N. Razak, M.N.A. Hamid,

- S.L. Teong, Effect of different stent configurations using Lattice Boltzmann method and particles image velocimetry on artery bifurcation aneurysm problem, *Journal of theoretical biology*, 433 (2017) 73-84.
- [23] B. Czaja, G. Závodszy, V. Azizi Tarksalooeyeh, A. Hoekstra, Cell-resolved blood flow simulations of saccular aneurysms: effects of pulsatility and aspect ratio, *Journal of The Royal Society Interface*, 15(146) (2018) 20180485.
- [24] H.H. Afrouzi, M. Ahmadian, M. Hosseini, H. Arasteh, D. Toghraie, S. Rostami, Simulation of blood flow in arteries with aneurysm: Lattice Boltzmann Approach (LBM), *Computer Methods and Programs in Biomedicine*, 187 (2020) 105312.
- [25] H. Wang, T. Krüger, F. Varnik, Effects of size and elasticity on the relation between flow velocity and wall shear stress in side-wall aneurysms: A lattice Boltzmann-based computer simulation study, *PLoS One*, 15(1) (2020) e0227770.
- [26] M. Löw, K. Perktold, R. Raunig, Hemodynamics in rigid and distensible saccular aneurysms: a numerical study of pulsatile flow characteristics, *Biorheology*, 30(3-4) (1993) 287-298.
- [27] K. Perktold, T. Kenner, D. Hilbert, B. Spork, H. Florian, Numerical blood flow analysis: arterial bifurcation with a saccular aneurysm, *Basic research in cardiology*, 83(1) (1988) 24-31.
- [28] K. Perktold, R. Peter, M. Resch, Pulsatile non-Newtonian blood flow simulation through a bifurcation with an aneurysm, *Biorheology*, 26(6) (1989) 1011-1030.
- [29] B.B. Lieber, A.P. Stancampiano, A.K. Wakhloo, Alteration of hemodynamics in aneurysm models by stenting: influence of stent porosity, *Annals of biomedical engineering*, 25(3) (1997) 460-469.
- [30] X. He, L.-S. Luo, Lattice Boltzmann model for the incompressible Navier–Stokes equation, *Journal of statistical Physics*, 88(3) (1997) 927-944.
- [31] R. Benzi, S. Succi, M. Vergassola, The lattice Boltzmann equation: theory and applications, *Physics Reports*, 222(3) (1992) 145-197.
- [32] Z. Guo, B. Shi, N. Wang, Lattice BGK model for incompressible Navier–Stokes equation, *Journal of Computational Physics*, 165(1) (2000) 288-306.
- [33] S. Succi, *The lattice Boltzmann equation: for fluid dynamics and beyond*, Oxford university press, 2001.
- [34] M. Sukop, D.T. Thorne, Jr. *Lattice Boltzmann Modeling Lattice Boltzmann Modeling*, (2006).
- [35] W. Nichols, M. O'Rourke, *McDonald's Blood Flow in Arteries* (Lea & Febiger, Philadelphia, PA), in, 1990.
- [36] A. Dupuis, From a lattice Boltzmann model to a parallel and reusable implementation of a virtual river, Citeseer, 2002.
- [37] A.R. Mantha, G. Benndorf, A. Hernandez, R.W. Metcalfe, Stability of pulsatile blood flow at the ostium of cerebral aneurysms, *Journal of biomechanics*, 42(8) (2009) 1081-1087.
- [38] K. Baráth, F. Cassot, D.A. Rüfenacht, J.H. Fasel, Anatomically shaped internal carotid artery aneurysm in vitro model for flow analysis to evaluate stent effect, *American Journal of Neuroradiology*, 25(10) (2004) 1750-1759.
- [39] Y.H. Kim, X. Xu, J.S. Lee, The effect of stent porosity and strut shape on saccular aneurysm and its numerical analysis with lattice Boltzmann method, *Annals of biomedical engineering*, 38(7) (2010) 2274-2292.
- [40] L. Bussel, V. Rayz, C. McCulloch, A. Martin, G. Acevedo-Bolton, M. Lawton, R. Higashida, W.S. Smith, W.L. Young, D. Saloner, Aneurysm growth occurs at region of low wall shear stress: patient-specific correlation of hemodynamics and growth in a longitudinal study, *Stroke*, 39(11) (2008) 2997-3002.
- [41] M. Ohta, S.G. Wetzel, P. Dantan, C. Bachelet, K.O. Lovblad, H. Yilmaz, P. Flaud, D.A. Rüfenacht, Rheological changes after stenting of a cerebral aneurysm: a finite element modeling approach, *Cardiovascular and interventional radiology*, 28(6) (2005) 768-772.
- [42] S. Kondo, N. Hashimoto, H. Kikuchi, F. Hazama, I. Nagata, H. Kataoka, Cerebral aneurysms arising at nonbranching sites: an experimental study, *Stroke*, 28(2) (1997) 398-404.
- [43] M. Shojima, M. Oshima, K. Takagi, R. Torii, M. Hayakawa, K. Katada, A. Morita, T. Kirino, Magnitude and role of wall shear stress on cerebral aneurysm: computational fluid dynamic study of 20 middle cerebral artery aneurysms, *Stroke*, 35(11) (2004) 2500-2505.
- [44] T.-M. Liou, S.-N. Liou, Pulsatile flows in a lateral aneurysm anchored on a stented and curved parent vessel, *Experimental Mechanics*, 44(3) (2004) 253-260.
- [45] S. Yu, J. Zhao, A steady flow analysis on the stented and non-stented sidewall aneurysm models, *Medical engineering & physics*, 21(3) (1999) 133-141.
- [46] R. Ouared, B. Chopard, Lattice Boltzmann simulations of blood flow: non-Newtonian rheology and clotting processes, *Journal of statistical physics*, 121(1) (2005) 209-221.
- [47] R.L. Sahjapaul, M.M. Abdulhak, C.G. Drake, R.R. Hammond, Fatal traumatic vertebral artery aneurysm rupture: Case report, *Journal of neurosurgery*, 89(5) (1998) 822-824.

HOW TO CITE THIS ARTICLE

M. Ahangari, M. Rezazadeh, *Numerical Simulation of Blood Flow in a Stented Aneurysm Using Lattice Boltzmann Method*, *AUT J. Mech Eng.*, 6(2) (2022) 229-248.

DOI: [10.22060/ajme.2022.20044.5987](https://doi.org/10.22060/ajme.2022.20044.5987)

